

ARMY RESEARCH LABORATORY



Unique Aspects of Micromechanics in Ballistic Penetration

by P. W. Kingman

ARL-TR-1412

July 1997

DTIC QUALITY INSPECTED 3

Approved for public release; distribution is unlimited.

19970912 156

The findings in this report are not to be construed as an official Department of the Army position unless so designated by other authorized documents.

Citation of manufacturer's or trade names does not constitute an official endorsement or approval of the use thereof.

Destroy this report when it is no longer need. Do not return it to the originator.

Army Research Laboratory

Aberdeen Proving Ground, MD 21005-5066

ARL-TR-1412

July 1997

Unique Aspects of Micromechanics in Ballistic Penetration

P. W. Kingman

Weapons and Materials Research Directorate, ARL

DTIC QUALITY INSPECTED 3

Approved for public release; distribution is unlimited.

Abstract

Ballistic experiments with tungsten penetrators composed of single crystals have been used to specify and constrain deformation modes in order to elucidate the role of flow and deformation mechanisms in penetration. The large differences in penetrator performance as a function of crystal symmetry are interpreted in terms of the structures observed and the basic deformation modes implied. The results suggest in very general terms the interactive role of material deformation parameters. The superior performance of the [001] orientation is attributed to the combination of yield strength with an unusually smooth lamellar flow after failure initiates. In contrast, the high yield strength of the [111] crystal is offset by the dissipation of energy in less efficient flow mechanisms and microstructural evolution. The analysis has implications for approaches to optimizing penetrator design through tailored materials and microstructures.

Acknowledgments

The writer wishes to acknowledge supportive and stimulating discussions with colleagues, particularly W. Bruchey, R. Herring, and E. Horwath, and laboratory support provided by D. MacKenzie.

INTENTIONALLY LEFT BLANK.

Table of Contents

	<u>Page</u>
Acknowledgments	iii
List of Figures	vii
1. Introduction	1
2. Experimental Approach	2
3. Experimental Results	3
3.1 [110] Penetrator	3
3.2 [111] Penetrator	5
3.3 [001] Penetrator	8
4. Discussion	13
5. Conclusion	15
6. References	17
Distribution List	19
Report Documentation Page	25

INTENTIONALLY LEFT BLANK.

List of Figures

<u>Figure</u>	<u>Page</u>
1. Results of Ballistic Tests Against Semi-Infinite RHA	2
2. Axial Section of [110] Penetrator, Showing Remnant Crystal and Flow Pattern	4
3. Layer Structure in Extrusion Tube of [110] Penetrator	4
4. Axial Section: Wavy Appearance of Exfoliations in [110] Extrusion Tube	6
5. Axial Section of [111] Penetrator: Flow Line Patterns and Internal Bands Near Lower Right Corner. Inset: Schematic of Residual	6
6. X-ray Analysis of Separated Crystal Segment Ahead of the [111] Residual Rod	7
7. Stereograms of Diffraction Patterns Taken in Sequence Across [001] Peripheral Flow Region	9
8. Partial Axial Section of [100] Penetrator With Orientation Analysis for Selected Regions	11
9. Convex Surface of [100] Penetrator Fragment (nose down): (a) Overview; (b) Tabular Packets; (c) Diffraction Pattern	12

INTENTIONALLY LEFT BLANK.

1. Introduction

The material flow mechanisms occurring under ballistic regimes exert a strong influence on penetration performance. Directional properties of materials have previously been recognized as a factor in the penetration process, but understanding of their actual role has been severely limited by the complexities of both mechanics and materials.

In a prior series of experiments at the U.S. Army Research Laboratory (ARL), tungsten rods machined from crystals at specified orientations were fired into semi-infinite rolled homogeneous armor [1]. The rationale for experiments with single crystals is that effects of penetrator geometry, ballistic conditions, and material parameters such as composition, density, grain size, etc., can be minimized. All specimens can be completely identical except for the internal (crystallographic) symmetry. Crystal symmetry is fundamental in determining the microstructural initiation and modes of material flow in crystalline materials, and at high symmetry the imposed constraints are stringent and specific. While single crystals may have limited practical application, well-specified experiments can be of great value in isolating and understanding the fundamental role of various deformation modes and their constraints.

The ballistic experiments have been described previously [1]. Figure 1 graphically summarizes the results. Each crystal rod had a selected unique crystallographic direction parallel to the penetrator axis. The observed results are a strong function of crystallographic symmetry, and in contrast with quasi-static stress-strain tests, the $[111]$ (three-fold symmetry axis) single crystal was not the best performer. The $[001]$ (four-fold symmetry axis) rod actually exceeded current tungsten heavy alloy penetrators and approached the performance of depleted uranium [1].

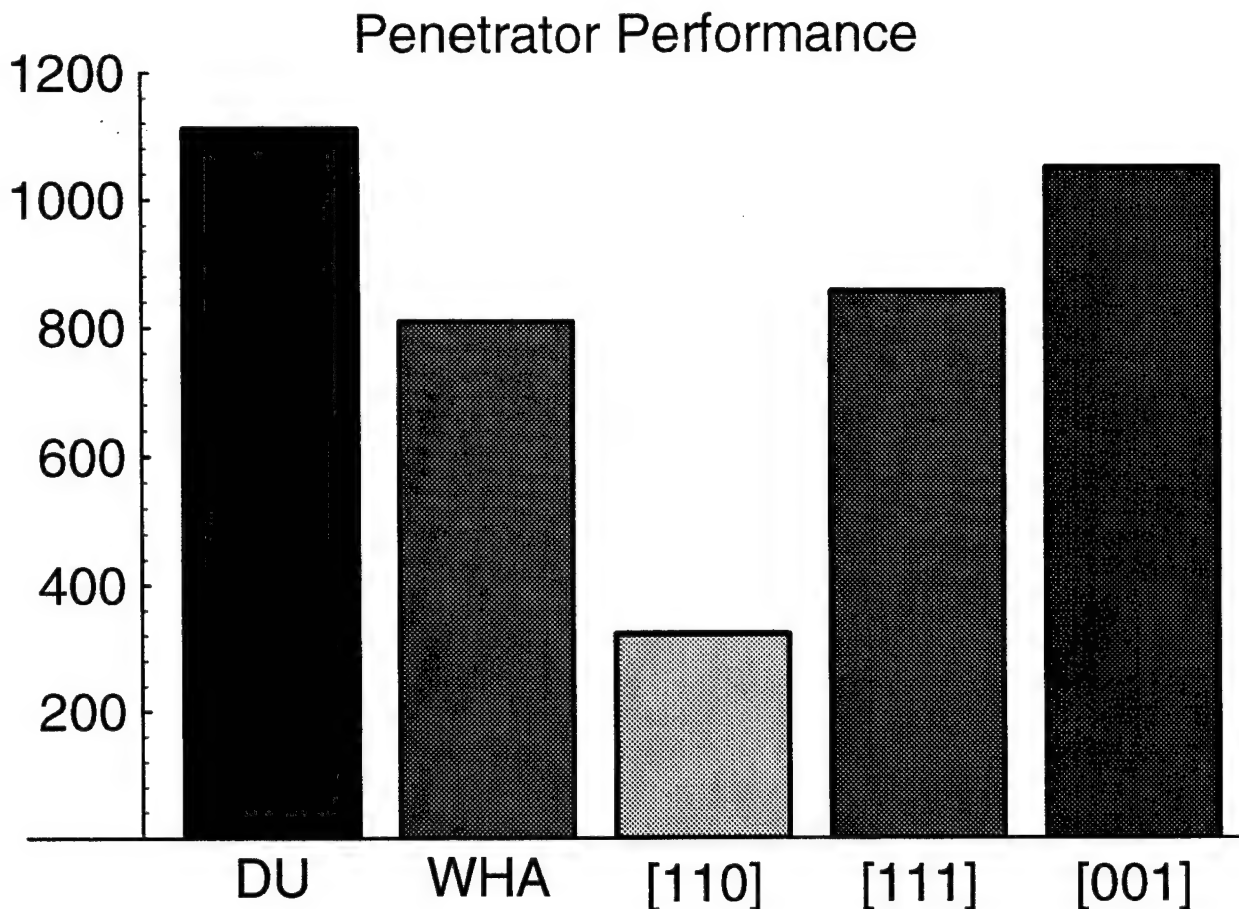


Figure 1. Results of Ballistic Tests Against Semi-Infinite RHA.

2. Experimental Approach

Axial sections of the targets demonstrated the effects of crystallographic orientation on the general flow pattern [1, 2]. The residual back end of the penetrator, typically about one diameter (~6 mm) in length, remained at the bottom of the penetration cavity surrounded by a thin layer of flowed material that extended back along the cavity walls to form a continuous hollow tube with a pattern of scroll-like foliations on the inner surface. Details of the final residual shape, the general appearance of the internal foliations, and the geometry and surface characteristics of the penetration tunnel differed for each crystal orientation, suggesting that the substantial differences in macroscopic penetration behavior originate in microscopic factors governing the initiation and continuation of material flow in the lattice.

Extensive characterization of the penetrator remnants was performed, utilizing optical microscopy and a variety of electron-optical and diffraction techniques. Diffraction data provide a basis for analyzing crystal orientation, lattice inhomogeneity (localized bending and substructure), recrystallization, grain size, preferred orientation, etc. A diffraction pattern from a small region of a single crystal can be analyzed to indicate the orientation of that region relative to the specimen axis, and visual features of the pattern can provide valuable qualitative information about the lattice distortion. The following discussion focuses primarily on the interpretation of the diffraction-based information as a key in bringing together all of the observations to form a coherent picture of the deformation process for each of these orientations.

3. Experimental Results

3.1 [110] Penetrator. This residual penetrator was completely recrystallized except for a small region at one corner of the back end (Figure 2). The material in the etched band structure is polycrystalline, and the Debye-Scherrer (D-S) rings from various regions indicated a variety of substructures ranging from sharp, equiaxed recrystallized grains to broad cold-worked rings, generally with strong texture. The rear surface of the rod was a mass of irregular surfaces, implying that the residual rod was heavily cracked and fragmented. The small remaining crystal fragment was tilted and deformed, so no useful orientation information could be obtained. The bands and cracks (probably originally axial) in the upper right portion of Figure 2 are thought to have initiated early in the process, followed later by laminar flow with extensive recrystallization. Although verification by diffraction was not possible, the appearance of the bands suggests twins, which would agree with observations by other workers [3, 4]. Figure 3 is a scanning micrograph of the layered structure in the extrusion tube. Some layers consist of relatively equiaxed grains and intergranular fractures, while the middle layer contains an extended region of cleavage. This microstructure agrees well with the flow pattern seen in Figure 2: some lamellae, possibly twin bands, developed a textured substructure which cleaved, while the surrounding material eventually recrystallized into equiaxed grains, resulting in intergranular fracture. The varied structure and appearance of the D-S rings in X-ray diffraction patterns from

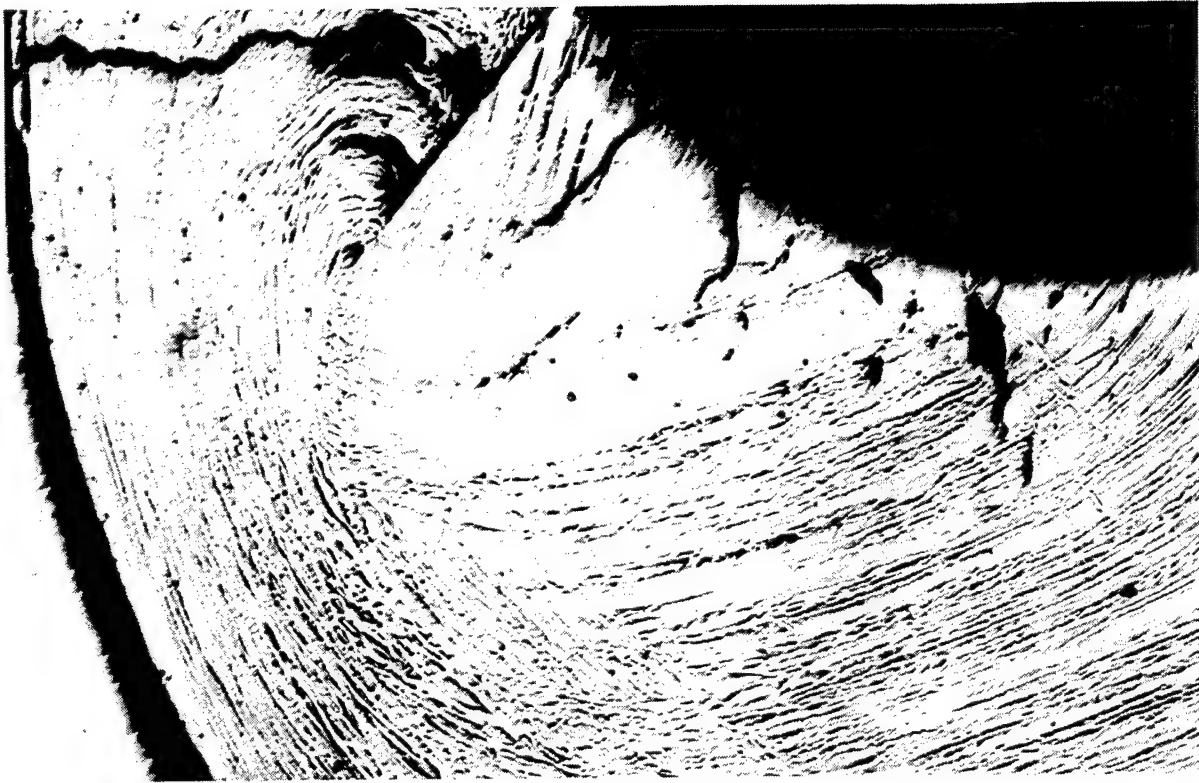


Figure 2. Axial Section of [110] Penetrator, Showing Remnant Crystal and Flow Pattern.

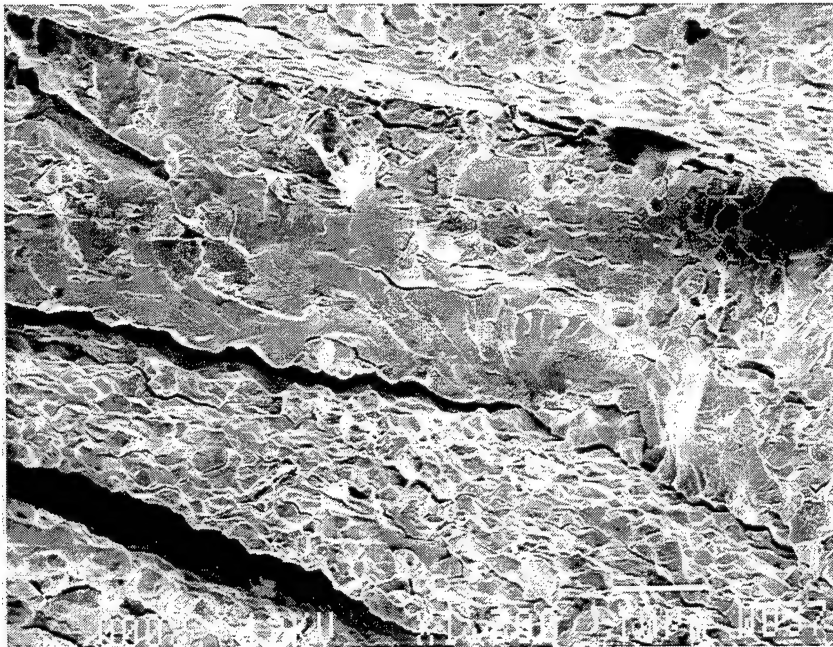


Figure 3. Layer Structure in Extrusion Tube of [110] Penetrator.

this residual also support that interpretation. The overall flow patterns and general appearance of the [110] extrusion tube are quite different from those of other orientations. The frond-like shape of the foliations suggests extensive ductile flow at this stage of the process (Figure 4).

3.2 [111] Penetrator. An axial section through the [111] residual penetrator is shown in Figure 5. Diffraction patterns showed that the well-defined, blunt-nosed residual rod (schematic inset in Figure 5) is a single crystal, with some uniform lattice distortion but little net lattice rotation. Material in the flowed regions was primarily polycrystalline, with some lamellar bands surrounded by regions of equiaxed recrystallized grains. A few relatively large lamellae, mostly embedded directly ahead of the residual rod, were still single crystals, although severely bent and deformed. These regions appear schematically below the residual crystal in the Figure 5 inset. Figure 6 shows a series of diffraction patterns from the largest crystal fragment. As a reference, the X-ray pattern at point (a) is typical of the main body of the residual rod. Diffraction patterns from points (b), (c), and (d), all within the largest fragment, showed heavily textured rings along with broad, structured discrete reflections. The crystal orientation changed continuously from point (b) to point (d). It appears that the separated segment was in the process of being forced out of the way of the oncoming rod, surrounded by material previously recrystallized.

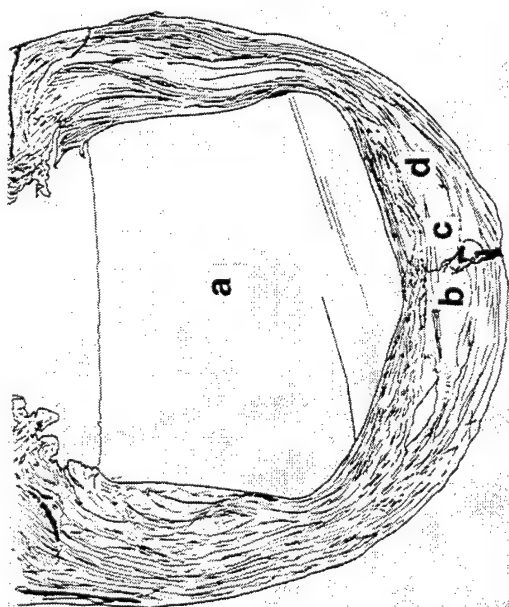
The precise nature of the few narrow bands appearing in the residual crystal could not be determined, but close examination suggests that they are flow bands whose propagation separates a crystal segment from the main rod. In the micrograph of Figure 5, a pair of closely spaced bands appears in the lower right corner. On the far right are layers of material that has already been discarded and forced out of the path of the rod. Just above the tip of the band is a small void between the rod and the discarded material, possibly opened up as the segment in the process of discard began to move to the right. We can infer that the segment below the band is just beginning to separate, the deformed and partially recrystallized region embedded directly below the rod resulted from a preceding discard, and the entire continuous layer of material surrounding the residual and extending to form the hollow tube is the result of a succession of such events.



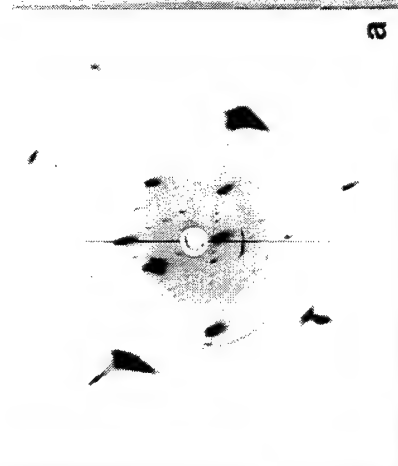
Figure 4. Axial Section: Wavy Appearance of Exfoliations in [110] Extrusion Tube.



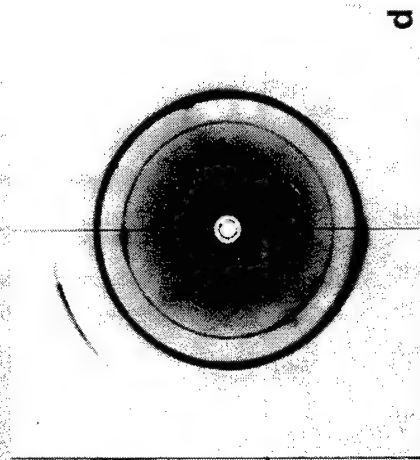
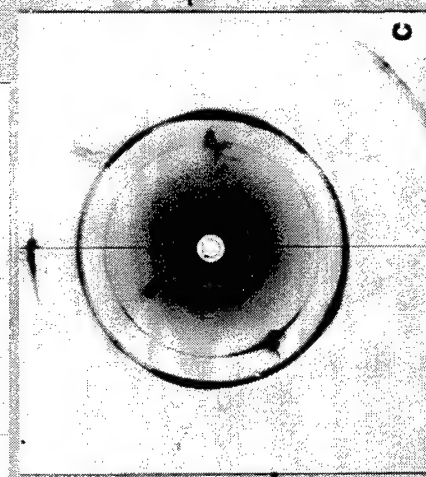
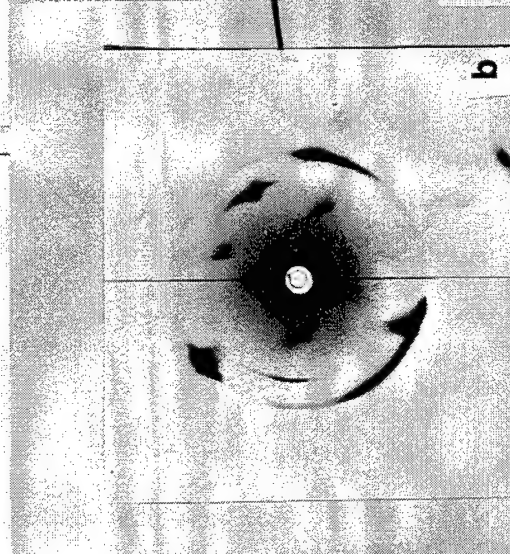
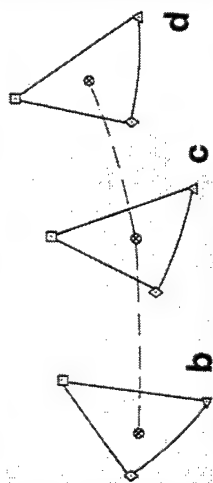
Figure 5. Axial Section of [111] Penetrator: Flow Line Patterns and Internal Bands Near Lower Right Corner. Inset: Schematic of Residual.



(Right) Reorientation of separated single crystal segment during radial flow at front of penetrator.



(Above) orientation of observation surface.
(Left) Diffraction pattern from center of $[111]$ residual rod (location a).



Diffraction patterns from locations a), b), c), in single crystal fragment embedded in flow ahead of remanent residual rod.

Figure 6. X-ray Analysis of Separated Crystal Segment Ahead of the $[111]$ Residual Rod.

3.3 [001] Penetrator. Contrasting with the [111] rod, optical micrographs of an axial section of the [001] penetrator showed no clearly outlined rod remnant. Instead, there is an assemblage of blocky segments defined by large cracks, and throughout much of the sample there occurs a fine-scale ($\sim 100\ \mu\text{m}$) network of narrow, straight crack segments intersecting at right angles (Figure 7). In the central residual rod, these cracks are parallel and perpendicular to the rod axis, but in the peripheral regions they become respectively radial and parallel to the cavity interface. On the left side of the extrusion tube, this rectangular pattern could be observed within the layers and exfoliations, while on the opposite side there appeared to be sequences of voids. X-ray patterns showed the persistence of discrete crystal reflections throughout the entire nose of the penetrator and well into the extrusion tube. In the residual rod remnant, the diffraction pattern was always sharp and well-defined, but even in the macroscopically flowed regions, discrete diffraction spots could be easily distinguished. Extensive analysis throughout the specimen established that the fine cracks were parallel to {001} cleavage planes in all cases. Where the cracks continuously varied in direction, the crystal orientation also continuously rotated, as shown by the sequence of orientations at the bottom of Figure 7 (the dot on each stereogram is the pole of the observation surface). These orientations were determined from a step-sequence of X-rays across the boxed region. The trace of the (001) plane (the lower edge of the standard triangle) exactly matches the crack direction with virtually no change in the appearance of the diffraction pattern except for rotation. Along the penetrator axis directly ahead of the residual rod, the orientation was maintained and the spots were uniformly broadened without asterism. The only exceptions occurred when the diffracting region included the immediate edges of large cracks, where patterns exhibited asterism and D-S rings from recrystallized material at the interface, and at the outer surface of the sample, where a thin layer of deformed material also produced D-S rings.

Along the left edge of the penetrator, lattice rotation can be documented continuously from the nose back into the hollow extrusion tube for several rod diameters without discontinuity, until the discrete spots finally disappear in strongly textured D-S patterns.

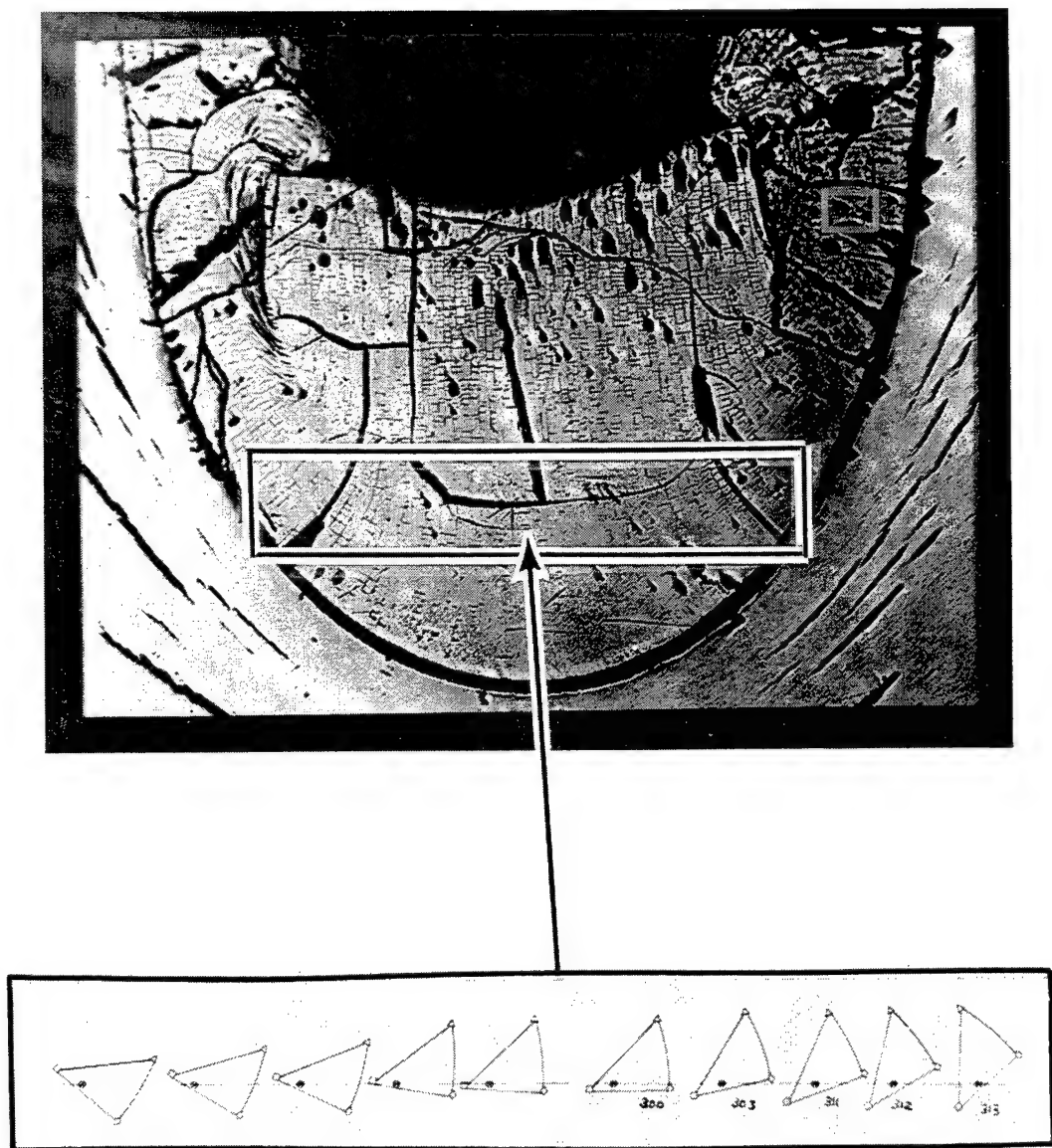


Figure 7. Stereograms of Diffraction Patterns Taken in Sequence Across [100] Peripheral Flow Region.

In the upper right corner of Figure 7, the microstructure appears inconsistent with the remainder of the sample, since the crack network is not evident. This region is shown in more detail in Figure 8a. X-ray analysis showed that above the severe inhomogeneity occurring adjacent to the residual rod, the lattice orientation abruptly changes by about 30° , so that the (001) cleavage plane is no longer normal to the rod axis. The void-like features occur because the cuboids tilt into the observation surface, and at many locations small segments were extracted during preparation. The micrograph in Figure 8 shows the changing crack patterns. On the left is a typical diffraction pattern from location "A" and the related stereogram. The dot is the pole of the observation surface, and the (100) plane is horizontal and nearly normal to the observation surface. On the right are (upper) the stereogram for region "B" and a sequence of stereograms from a traverse across the transition region "C." The accompanying typical diffraction pattern corresponds to the "double" stereogram plotted from the opposite ends of each elongated diffraction spot. The orientation of the crack patterns in the transition region can be seen to change in parallel with the (100) trace in the stereograms, which indicate (as does the shape of the spots) a single-axis rotation about the observation normal.

Examination of a second [001] penetrator further elucidated the nature of this rotation and the true three-dimensional character of the deformation process. This penetrator cracked during flight and impacted the target in two closely spaced coaxial segments, and thus the residual did not have full integrity. After sectioning, most of the residual dropped out intact, leaving a partial shell of deformed layers adhered to the concave surface at the bottom of the penetration tunnel in the target block. Figure 9a is a scanning image of the convex surface of this extracted fragment at low magnification (nose pointed down). The convex surface appears covered with tabular rectangular packets, often rotated relative to one another (Figure 9b). Although a thin surface layer was deformed and partially recrystallized, discrete diffraction spots were distinctly visible in these packets (Figure 9c). It appears that material flow in the [001] crystals is not purely radial but that the flow packets of {001} layers also have a rotational degree of freedom about the normal to the packet. This would imply a very substantial degree of independence for these entities after cleavage. The rectangular edges of the packets also appear to be defined by {001} cleavage planes, but this could not be directly confirmed.

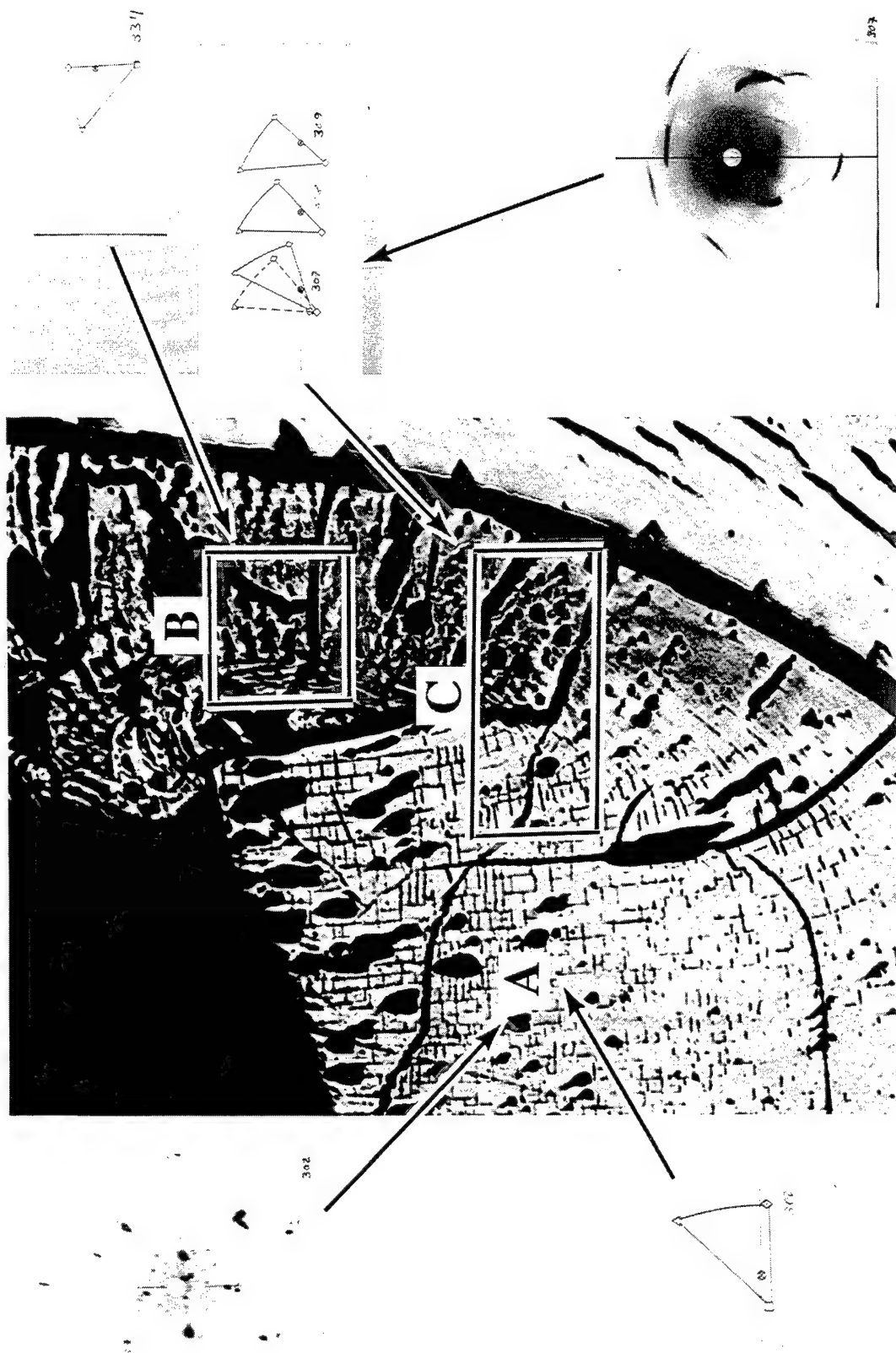


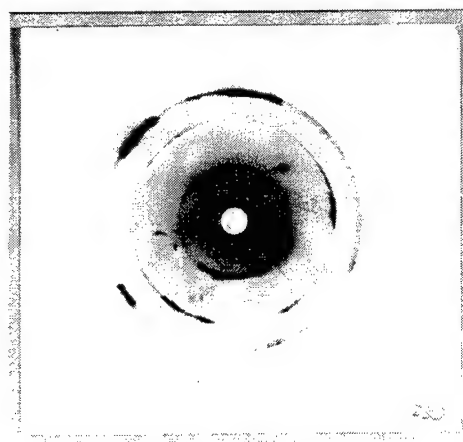
Figure 8. Partial Axial Section of [100] Penetrator With Orientation Analysis for Selected Regions.




Down



B



C

Figure 9. Convex Surface of [100] Penetrator Fragment (nose down): (a) Overview; (b) Tabular Packets; (c) Diffraction Pattern.

4. Discussion

From the experimental observations, it is evident that the operative microstructural processes are unique for each symmetry orientation.

In the [111] crystal, three $\langle 111 \rangle$ directions occur symmetrically at 70.5° from the rod axis. Resolved shear stresses on dislocations having these three Burgers vectors are thus relatively low, resulting in a high yield strength, while ample generation of dislocations available for interaction enhances work hardening. The tip of the residual is blunt, and it appears that relatively thick segments of material separate from the rod along narrow shear localizations and are forced outward toward the cavity walls along the blunt surface angle of the rod remnant while undergoing extensive working and recrystallization. The three-dimensional geometry of the separating segments is undetermined, but the cavity walls, which appear wavy in the axial section, are actually covered with discrete craters rather than having a circumferential undulation. All of these features suggest a less-than-smooth process. This sample was also the only one to possess a distinct surface layer of diffused iron from the target block, as well as iron solidified inside open cracks, indicating substantial heat generation during penetration. All of these observations suggest relatively greater diversion of forward kinetic energy into heating, hot working, and microstructure evolution as radial mass transfer and penetrator erosion take place.

For the [110] orientation, both imaging and diffraction results indicate that the penetrator material has repeatedly recrystallized, deformed, and recrystallized again. Classically, [110] bcc crystals have a high yield strength but do not work harden because the necessary dislocation reactions are unavailable due to symmetry. At high impact velocities, twins may occur [3, 4]. The bands seen in the micrographs were too fine and inhomogeneous to analyze by X-ray diffraction, but the possibility that both twins and axial cracks occurred early in the deformation process would agree with other observations on bcc materials. The consequent loss of integrity could account for the poor penetration in spite of the ductile flow.

In the [001] penetrator, with four-fold symmetry, all four $\langle 111 \rangle$ directions are equally stressed, creating large numbers of dislocations able to react with one another. One possible reaction is the Cottrell reaction [5]

$$\frac{1}{2} a [111] + \frac{1}{2} a [\bar{1}\bar{1}\bar{1}] \rightarrow a [100], \quad (1)$$

which produces a sessile dislocation. This sessile dislocation is associated with the initiation of {001} cleavage cracks in bcc crystals oriented with a tensile stress axis along the [001] direction [5, 6].

Under impact conditions it can be reasonably speculated that a large distribution of dislocations would immediately be created and move only a short distance before interacting to create an extended array of sessile dislocations. This array would then inhibit work hardening and create nucleation sites for cleavage cracks as the deviatoric stresses increase and material flow is initiated. The smooth lamellar bending and shear, along with the relative absence of substructure, complex lattice distortion, and recrystallization in X-ray patterns from much of the peripheral flow region, indicate that relatively little work hardening occurs in the [001] penetrator. In contrast with the [111] hole profile, the [001] penetration tunnel is narrow and exceptionally smooth, and there is less material interaction between the penetrator and the target. Rather than discontinuously shedding finite material segments, the [001] rod is postulated to flow by a smooth quasi-continuous process in which small, finite lattice elements defined by (001) cleavage planes undergo a combination of lamellar bending and rotation during flow with little internal disturbance. This is a highly efficient process, permitting maximum partition of energy into forward motion. The persistence of the rectangular crack pattern through the curved foliations in the extrusion tube is strong evidence that lamellar flow of finite entities with minimal lattice disruption is the dominant deformation mode and that continuous reorientation of these discrete entities was complete before any recrystallization occurred. The observed rotation of the lamellar packets also suggests a substantial degree of independence for these entities during deformation.

Recently, ballistic experiments have been done with oriented polycrystals composed of individual grains having a symmetry axis oriented along the penetrator axis, with unconstrained rotations about the axis [7]. Differences between the major symmetry directions still exist but are smaller, and the [001] specimens perform less advantageously. Since the (001) cleavage is still theoretically normal to the axis in all grains, it is not clear whether the decrease in performance derives solely from mismatch obstacles to direct radial shear or whether the additional rotation of the packet about the normal to the cleavage plane may be essential to easy flow, and may be constrained in the polycrystal.

5. Conclusion

Ballistic penetration tests using rods machined from tungsten single crystals at specified orientations have shown that crystallography, which governs microstructural failure and flow mechanisms, is a strong determinant of penetration behavior. As previously noted by Magness and others [8, 9], classical quasi-static data do not necessarily imply similar performance in ballistic penetration. The excellent performance of the [001] orientation has been shown to result from a unique deformation mode in which work hardening is suppressed and flow initiates at microscopic inhomogeneities. In this mode, small but distinct crystal entities shear and flow with minimal internal deformation. Although adiabatic shear does not occur, this mode similarly activates an energetically efficient, uniform flow. Maximizing the fraction of total energy partitioned into forward penetration results in a deep, narrow, smooth-walled penetration cavity similar to that produced by depleted uranium (DU).

Single-crystal experiments provide a unique opportunity to specify highly constrained deformation modes. Basic material mechanisms are thus isolated without introducing additional material variables. Understanding these fundamental mechanisms will lead to a basis for designing novel materials and composites for future application.

INTENTIONALLY LEFT BLANK.

6. References

1. Bruchey, W. J., E. J. Horwath, and P. W. Kingman. "Orientation Dependence of Deformation and Penetration Behavior of Tungsten Single-Crystal Rods." *Tungsten and Tungsten Alloys, Recent Advances*, edited by A. Crowson and E. Chen, Warrendale, PA: TMS, 1991.
2. Bruchey, W. J., R. A. Herring, P. W. Kingman, and E. J. Horwath. "Deformation Mechanisms in Tungsten Single Crystals in Ballistic Impact Experiments." *High Strain Rate Behavior of Refractory Metals and Alloys*, edited by R. Asfahni et al., Warrendale, PA: TMS, 1992.
3. Vecchio, K. Private communication. University of California - San Diego, San Diego, CA, 1993.
4. Subhash, G., Y. J. Lee, and G. Ravichandran. "Plastic Deformation of CVD Textured Tungsten-II. Characterization." *Acta Metallurgica et Materialia*, vol. 42, pp. 331–340, 1994.
5. Cottrell, A. H. "Theory of Brittle Fracture in Steel and Similar Metals." *Transactions of the AIME*, vol. 212, pp. 192–203, 1958.
6. Carrington, W., K. F. Hale, and D. McLean. "Arrangement of Dislocations in Iron." *Proceedings of the Royal Society of London, Series A, Mathematical and Physical Sciences*, vol. 259, pp. 203–227, 1960.
7. Leonard, W., L. Magness, M. Chang, and D. Kapoor. "The Performance of Oriented Columnar Grained Polycrystalline Tungsten Penetrators." *Proceedings of the 16th International Ballistics Symposium*, vol. 3, pp. 617–626, 1996.
8. Magness, L. S. "Properties and Performance of KE Penetrator Materials." *Tungsten and Tungsten Alloys*, Princeton, NJ: Metal Powder Industries Federation, pp. 15–22, 1992.
9. Magness, L. S., and T. S. Farrand. "Deformation Behavior and Its Relationship to the Penetration Performance of High-Density KE Penetrator Materials." *Proceedings of the 1990 Army Science Conference*, pp. 465–479, 1991.

INTENTIONALLY LEFT BLANK.

NO. OF
COPIES ORGANIZATION

2 DEFENSE TECHNICAL
INFORMATION CENTER
DTIC DDA
8725 JOHN J KINGMAN RD
STE 0944
FT BELVOIR VA 22060-6218

1 HQDA
DAMO FDQ
DENNIS SCHMIDT
400 ARMY PENTAGON
WASHINGTON DC 20310-0460

1 CECOM
SP & TRRSTRL COMMCTN DIV
AMSEL RD ST MC M
H SOICHER
FT MONMOUTH NJ 07703-5203

1 PRIN DPTY FOR TCHNLGY HQ
US ARMY MATCOM
AMCDCG T
M FISETTE
5001 EISENHOWER AVE
ALEXANDRIA VA 22333-0001

1 PRIN DPTY FOR ACQUSTN HQS
US ARMY MATCOM
AMCDCG A
D ADAMS
5001 EISENHOWER AVE
ALEXANDRIA VA 22333-0001

1 DPTY CG FOR RDE HQS
US ARMY MATCOM
AMCRD
BG BEAUCHAMP
5001 EISENHOWER AVE
ALEXANDRIA VA 22333-0001

1 ASST DPTY CG FOR RDE HQS
US ARMY MATCOM
AMCRD
COL S MANESS
5001 EISENHOWER AVE
ALEXANDRIA VA 22333-0001

NO. OF
COPIES ORGANIZATION

1 DPTY ASSIST SCY FOR R&T
SARD TT F MILTON
THE PENTAGON RM 3E479
WASHINGTON DC 20310-0103

1 DPTY ASSIST SCY FOR R&T
SARD TT D CHAIT
THE PENTAGON
WASHINGTON DC 20310-0103

1 DPTY ASSIST SCY FOR R&T
SARD TT K KOMINOS
THE PENTAGON
WASHINGTON DC 20310-0103

1 DPTY ASSIST SCY FOR R&T
SARD TT B REISMAN
THE PENTAGON
WASHINGTON DC 20310-0103

1 DPTY ASSIST SCY FOR R&T
SARD TT T KILLION
THE PENTAGON
WASHINGTON DC 20310-0103

1 OSD
OUSD(A&T)/ODDDR&E(R)
J LUPO
THE PENTAGON
WASHINGTON DC 20301-7100

1 INST FOR ADVNCD TCHNLGY
THE UNIV OF TEXAS AT AUSTIN
PO BOX 202797
AUSTIN TX 78720-2797

1 DUSD SPACE
1E765 J G MCNEFF
3900 DEFENSE PENTAGON
WASHINGTON DC 20301-3900

1 USAASA
MOAS AI W PARRON
9325 GUNSTON RD STE N319
FT BELVOIR VA 22060-5582

<u>NO. OF</u> <u>COPIES</u>	<u>ORGANIZATION</u>
1	CECOM PM GPS COL S YOUNG FT MONMOUTH NJ 07703
1	GPS JOINT PROG OFC DIR COL J CLAY 2435 VELA WAY STE 1613 LOS ANGELES AFB CA 90245-5500
1	ELECTRONIC SYS DIV DIR CECOM RDEC J NIEMELA FT MONMOUTH NJ 07703
3	DARPA L STOTTS J PENNELLA B KASPAR 3701 N FAIRFAX DR ARLINGTON VA 22203-1714
1	SPCL ASST TO WING CMNDR 50SW/CCX CAPT P H BERNSTEIN 300 O'MALLEY AVE STE 20 FALCON AFB CO 80912-3020
1	USAF SMC/CED DMA/JPO M ISON 2435 VELA WAY STE 1613 LOS ANGELES AFB CA 90245-5500
1	US MILITARY ACADEMY MATH SCI CTR OF EXCELLENCE DEPT OF MATHEMATICAL SCI MDN A MAJ DON ENGEN THAYER HALL WEST POINT NY 10996-1786
1	DIRECTOR US ARMY RESEARCH LAB AMSRL CS AL TP 2800 POWDER MILL RD ADELPHI MD 20783-1145

<u>NO. OF</u> <u>COPIES</u>	<u>ORGANIZATION</u>
1	DIRECTOR US ARMY RESEARCH LAB AMSRL CS AL TA 2800 POWDER MILL RD ADELPHI MD 20783-1145
3	DIRECTOR US ARMY RESEARCH LAB AMSRL CI LL 2800 POWDER MILL RD ADELPHI MD 20783-1145
	<u>ABERDEEN PROVING GROUND</u>
2	DIR USARL AMSRL CI LP (305)

NO. OF
COPIES ORGANIZATION

3 CDR US ARO
ATTN J CHANDRA
A CROWSON
K IYER
PO BOX 12211
RESEARCH TRIANGLE PARK NC
27709-2211

3 DIR WL MNMW
ATTN W COOK
J FOSTER JR
TECH LIB
EGLIN AFB FL 32542-5434

2 DIR LANL
ATTN P DUNN
W HOGAN
PO BOX 1663 G770
LOS ALAMOS NM 87545

2 DIR LLNL
ATTN C CLINE
R GOGOLEWSKI
BOX 808
LIVERMORE CA 94550

1 BROWN UNIV
DIV OF ENGRNG
ATTN R CLIFTON
PROVIDENCE RI 02912

4 IAT
ATTN S BLESS
T KIEHNE
M J NORMANDIA
R SUBRAMANIAN
4030 2 W BRAKER LN
AUSTIN TX 78759-5329

3 JHU
DEPT OF MAT SCI
ATTN RE GREEN
R POND
J WINTER
MD HALL
34TH & CHARLES ST
BALTIMORE MD 21218

NO. OF
COPIES ORGANIZATION

2 JHU
DEPT OF MECH ENG
ATTN K HEMKER
K T RAMESH
LATROBE 104
34TH & CHARLES ST
BALTIMORE MD 21218

1 MICHIGAN TECH UNIV
DEPT OF MECH ENG
ATTN G SUBHASH
HOUGHTON MI 49931

1 PURDUE UNIV
DEPT OF MATLS ENGRNG
ATTN K BOWMAN
WEST LAFAYETTE IN 47907

2 SW RSRCH INSTI
ATTN C ANDERSON
J LANKFORD
PO DWR 28510
SAN ANTONIO TX 78228-0510

2 UNIV OF CA SAN DIEGO
DEPT OF APLD MCHNCS
& ENGRNG SCI B 010
ATTN M MEYER
K VECCHIO
LA JOLLA CA 92093

1 ADLEMAN ASSOC
ATTN C CLINE
3301 EL CAMINO REAL STE 280
ATHERTON CA 94027

3 BATTELLE PNL
ATTN G DUDDER
W GURWELL
R SHIPPELL
RICHLAND WA 99352

1 CONCURRENT TECH CORP
ATTN T MCCABE
1450 SCALP AVE
JOHNSTOWN PA 15904

NO. OF
COPIES ORGANIZATION

1 ZERNOW TECH SVC INC
ATTN L ZERNOW
425 W BENITA STE 208
SAN DIMAS CA 91773

ABERDEEN PROVING GROUND

39 DIR USARL
ATTN: AMSRL-WM-M, J MCCAULEY
AMSRL-WM-MA-CB,
R DOWDING
P WOOLSEY
AMSRL-WM-ME,
R ADLER
E CHIN
M WELLS
AMSRL-WM-T, W F MORRISON
AMSRL-WM-TA,
S BILYK
W BRUCHEY
G BULMASH
G FILBEY
W GILLICH
E HORWATH
Y HUANG
D MACKENZIE
H MEYER
E RAPACKI
W ROWE
AMSRL-WM-TC,
F GRACE
E KENNEDY
L MAGNESS
AMSRL-WM-TD
A M DEITRICH
K FRANK
T FARRAND
P KINGMAN (4 CP)
S SCHOENFELD
M SCHEIDLER
J WALTER
T WRIGHT
AMSRL-WM-MF,
S CHOU
D DANDEKAR
D GROVE
A RAJENDRAN
T WEERASOORIYA
AMSRL-WM-WD, L KECSKES

NO. OF
COPIES ORGANIZATION

2 CDR
DRA FRT HALSTEAD
ATTN A BENTLEY
M HOGWOOD
SEVENOAKS KENT TN14 7BP
UNITED KINGDOM

1 DIR MRL
ATTN R WOODWARD
PO BOX 50
ASCOT VALE VIC 3052
AUSTRALIA

INTENTIONALLY LEFT BLANK.

REPORT DOCUMENTATION PAGE			Form Approved OMB No. 0704-0188	
Public reporting burden for this collection of information is estimated to average 1 hour per response, including the time for reviewing instructions, searching existing data sources, gathering and maintaining the data needed, and completing and reviewing the collection of information. Send comments regarding this burden estimate or any other aspect of this collection of information, including suggestions for reducing this burden, to Washington Headquarters Services, Directorate for Information Operations and Reports, 1215 Jefferson Davis Highway, Suite 1204, Arlington, VA 22202-4302, and to the Office of Management and Budget, Paperwork Reduction Project(0704-0188), Washington, DC 20503.				
1. AGENCY USE ONLY (Leave blank)	2. REPORT DATE June 1997	3. REPORT TYPE AND DATES COVERED Final, March - August 1996		
4. TITLE AND SUBTITLE Unique Aspects of Micromechanics in Ballistic Penetration		5. FUNDING NUMBERS 61102AH43		
6. AUTHOR(S) P. W. Kingman				
7. PERFORMING ORGANIZATION NAME(S) AND ADDRESS(ES) U.S. Army Research Laboratory ATTN: AMSRL-WM-TA Aberdeen Proving Ground, MD 21005-5066		8. PERFORMING ORGANIZATION REPORT NUMBER ARL-TR-1412		
9. SPONSORING/MONITORING AGENCY NAMES(S) AND ADDRESS(ES)		10. SPONSORING/MONITORING AGENCY REPORT NUMBER		
11. SUPPLEMENTARY NOTES				
12a. DISTRIBUTION/AVAILABILITY STATEMENT Approved for public release; distribution is unlimited.		12b. DISTRIBUTION CODE		
13. ABSTRACT (Maximum 200 words) Ballistic experiments with tungsten penetrators composed of single crystals have been used to specify and constrain deformation modes in order to elucidate the role of flow and deformation mechanisms in penetration. The large differences in penetrator performance as a function of crystal symmetry are interpreted in terms of the structures observed and the basic deformation modes implied. The results suggest in very general terms the interactive role of material deformation parameters. The superior performance of the [001] orientation is attributed to the combination of yield strength with an unusually smooth lamellar flow after failure initiates. In contrast, the high yield strength of the [111] crystal is offset by the dissipation of energy in less efficient flow mechanisms and microstructural evolution. The analysis has implications for approaches to optimizing penetrator design through tailored materials and microstructures.				
14. SUBJECT TERMS micromechanics, anisotropy, ballistics, penetration, single crystal, tungsten		15. NUMBER OF PAGES 27		
		16. PRICE CODE		
17. SECURITY CLASSIFICATION OF REPORT UNCLASSIFIED	18. SECURITY CLASSIFICATION OF THIS PAGE UNCLASSIFIED	19. SECURITY CLASSIFICATION OF ABSTRACT UNCLASSIFIED	20. LIMITATION OF ABSTRACT UL	

INTENTIONALLY LEFT BLANK.

USER EVALUATION SHEET/CHANGE OF ADDRESS

This Laboratory undertakes a continuing effort to improve the quality of the reports it publishes. Your comments/answers to the items/questions below will aid us in our efforts.

1. ARL Report Number/Author ARL-TR-1412 (Kingman) Date of Report June 1997
2. Date Report Received _____
3. Does this report satisfy a need? (Comment on purpose, related project, or other area of interest for which the report will be used.) _____

4. Specifically, how is the report being used? (Information source, design data, procedure, source of ideas, etc.) _____

5. Has the information in this report led to any quantitative savings as far as man-hours or dollars saved, operating costs avoided, or efficiencies achieved, etc? If so, please elaborate. _____

6. General Comments. What do you think should be changed to improve future reports? (Indicate changes to organization, technical content, format, etc.) _____

CURRENT
ADDRESS

Organization

Name

E-mail Name

Street or P.O. Box No.

City, State, Zip Code

7. If indicating a Change of Address or Address Correction, please provide the Current or Correct address above and the Old or Incorrect address below.

OLD
ADDRESS

Organization

Name

Street or P.O. Box No.

City, State, Zip Code

(Remove this sheet, fold as indicated, tape closed, and mail.)
(DO NOT STAPLE)

DEPARTMENT OF THE ARMY

OFFICIAL BUSINESS

BUSINESS REPLY MAIL

FIRST CLASS PERMIT NO 0001,APG,MD

POSTAGE WILL BE PAID BY ADDRESSEE

DIRECTOR
US ARMY RESEARCH LABORATORY
ATTN AMSRL WM TA
ABERDEEN PROVING GROUND MD 21005-5066



NO POSTAGE
NECESSARY
IF MAILED
IN THE
UNITED STATES

